Nat. Volatiles & Essent. Oils, 2021; 8(4): 13478-13496

NVEO
Natural Volatiles & Essential Oils

Synthesis, Characterization and Biological Study of New Crown Ether Prodrugs as Anticancer Agents.

Marwan Majeed K. Al-Lammi [1*], Raheem Jameel M.[2], Layla Jasim Abbas[3]

[1,2,3]*University of Basrah, College of Pharmacy, Department of Pharmaceutical Chemistry, Basrah, Iraq.*

Abstract:

In the present work, new Schiff's bases prodrugs 4,4`-di[9-(2-hydroxyethoxy) methyl]-2-(methylidene amino)-1,9-dihydro-6H-purin-6-one- [6,7,9,10,17,18,20,21]- Octa hydro- [b, k] dibenzo [1,4,7,10,13,16] hexaoxacyclooctadecine, 4,4`-di-1-[3,4-dihydroxy-5-(hydroxymethyl) oxolan-2-yl]-4-[(E)-ethylideneamino] pyrimidin-2(1H)-one- [6,7,9,10,17,18,20,21]- Octa hydro- [b, k] dibenzo [1,4,7,10, 13, 16] hexaoxacyclooctadecine and 4,4`-di-5-[2-chloro-6-(methylideneamino)-9H-purin-9-yl]-2-(hydroxymethyl) oxolan-3-ol-[6,7,9,10,17,18,20,21]- Octa hydro- [b, k] dibenzo [1,4,7,10,13,16] hexaoxacyclooctadecine were designed by nucleophilic addition of primary amines and active carbonyl groups through a condensation reaction. These processes were started from the formylation reaction of dibenzo-18-crown-6-ether then linking of 4,4-diformyldibenzo-18-crown-6 ether with the desired nucleoside analogues (acyclovir, cytarabine and cladribine) to produce the previously mentioned prodrug A1, A2 and A3, respectively. These compounds were designed as carrier-mediated prodrugs to overcome some pharmaceutical and pharmacokinetic problems, improve physicochemical properties and provide structural modifications of the parent drugs to enhance their anticancer activities. The structures of the synthesized compounds were confirmed using UV, FT-IR spectroscopy, mass spectrometry, ^{1}H and ^{13}C NMR spectroscopy and some physiochemical properties. The prepared prodrugs offered high capacity to inhibit the proliferation of cancer cell lines in a concentration-dependent way when compared to the parent drugs.

Keywords: Crown ether, nucleoside analogues, Schiff's bases, anticancer activity.

Introduction:

However first crown ethers were reported by Luttringhaus in 1937, the history of macrocyclic compounds synthesis belong to 1967 [1]. Charles John Pedersen innovated an easy practical method for the first manufacturing of a variety of cyclic polyether compounds named "Crown

Ethers" [2]. Macrocyclic compounds (MCs) are organic compounds containing an acyclic ring of more than 12 atoms of growing interest in the field of supramolecular chemistry[3], a branch of chemistry coined by Jean-Marie Lehn in the 1970 which study of all types of intermolecular non-covalent bond formation in designed molecular systems[4] and inhibition of all challenging undergo during drug targets[5]. Host–guest chemistry using macrocyclic compounds as hosts because of their bioactivity [5] and structure-specific interactions of high selectivity which belong to highly symmetrical structures with an oligomeric molecular weight and mono-dispersity which possess a cavity in which they can accommodate guest molecules[3].

Crown ethers are subclass of cyclic ethers or macrocyclic polyethers containing (3-20) oxygen atoms separated by (2-3) carbon atoms with the general formula $(OCH_2CH_2)_n$. The central core of all crown ethers is a hydrophilic cavity of different sizes that can conciliate a metal ion coordinated to oxygen atoms of the ring, whereas the outer shell is hydrophobic, consisting of (C–H) bonds. The interaction between cation and electron lone pairs of the oxygen atoms on crown framwork enhanced cation stabilization and solvation as showen in **Figure (1).**

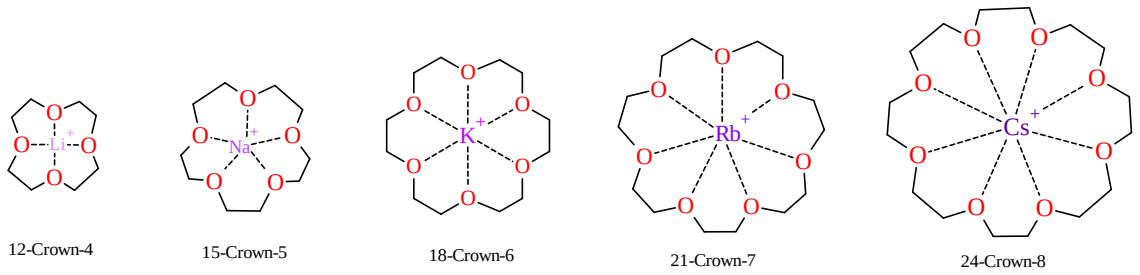

Figure (1): Complexation of crown ethers with selective metal cations.

Non-medicinal applications of crown ethers are involved synthetic and analytical applications. The synthetic applications are including some processes such as: esterification, saponification, anhydride formation, potassium permanganate oxidation, aromatic substitution reactions, elimination reactions, displacement reaction, generation of carbenes and furanones, resolution of racemic mixture, acetylation of secondary amines in presence of primary amine, heterocyclisation, benzoin condensation, photocynation and alkylation reactions , and in the field of synthetic biology as membrane anchors for DNA- controlled content mixing between liposomes [6]. The analytical applications of crown ethers are involved: determination of gold in geological samples, supercritical fluid extraction of trace metal from solids and liquids, oxidation

and determination of aldehydes , catalysis as phase transfer catalyst [7], chemical sensor for either recognition or quantification of analytes[8] or as stationary phase in the chromatography[9], as ion transport in biological system and in living cell imiging[8], in different studies and experiments in chemistry and nanotechnology applications[10].

Crown ethers are now being researched and used in a wide range of applications outside of chemistry. These compounds exhibit a variety of biological [11] and medicinal [12] properties. Most of the biological processes involve recognition, membrane transport, signal transduction, information storage, biocatalysis, reproduction and processing based on host-guest interactions such as charge transfer phenomena, dipole-dipole interactions, ion-dipole interactions, hydrogen bonding, and solvent effect, gives a predictable basis for the chemical structures designing that behaved the same mannar as chemical structures of complex in biological systems[13]. Crown ethers play an important role as targeting drug delivery systems[14],[15] due to the effects of macrocyclization upon target potency, selectivity and compound physicochemical properties[12]. Crown ethers in drug delivery systems is an intriguing concept, and much progress has been achieved in this area. They are ideal for transporting across membranes and interfering with many life systems due to their ionophoric characteristics. Crown ethers play an important role of as vesicles (liposomes and niosomes), in gene therapy as DNA vector, as ion transport carrier, as drug-targeting vectors, as nano-carrier, as Transthyretin Amyloidogenesis Inhibitors[16], as permeability enhancers for ocular drug delivery [17], have antimicrobial and antimutagenic activities, inhibition of protein synthesis in reticulocytes and to their antimutagenic activity, can reverse P-glycoprotein-mediated multidrug resistance in cancer cells[18] and play a pivotal role in the treatment of some mental disease such as Alzheimer's and parkinson's diseases.

Acyclovir, cytarabine and cladribine are nucleoside analogues primarily used as anticancer agents with some antiviral activities which classified according to the Biopharmaceutical Classification System (BCS), a model used to describe the solubility and permeability of drug, as class III/IV for acyclovir, class III for cytarabine and cladribine with some pharmaceutical and pharmacokinetic profile problems.

Schiff's base ligands are compounds carrying an imine or azomethine (–C=N–) functional group which were first synthesized in 1864 by German Chemist, Hugo Schiff through the condensation of aliphatic or aromatic primary amines and carbonyl compounds, aldehydes or ketones by nucleophilic addition forming a hemiaminal, followed by a dehydration to generate an imine [19],[20]. Schiff's base ligands have an interesting structure and electronic properties through the presence of a lone pair of electrons on sp^2 hybridized nitrogen of the azomethine group which act as binding site to form complexes with transition metal ions to be attached with various biomolecules like proteins and amino acids for antigerm activities through the formation of a hydrogen bond between the active centers of cell constituents in biological systems [21],[22] .

Materials and Methods

Materials

Dibenzo-18-crown ether (Hyper-chem, China), Acyclovir (Hyper-chem, China), Cytarabine (Pfizer, USA), Cladribine (Janssen, Korea), Trifluoroacetic acid (Alfa Aesar, U. K), Hexamethylene tetraamine (Sigma – Aldrich, Germany), Absolute ethanol (96%) (Sigma – Aldrich, Germany), Absolute methanol (Sigma – Aldrich, Germany), Chloroform (BDH, U. K), Glacial acetic acid (BDH, U. K), Dichloromethane anhydrous (Sigma – Aldrich, Germany), Ammonium hydroxide (Sigma – Aldrich, Germany), Dimethyl sulfoxide (Santacruz Biotechnology, USA), Fetal bovine serum (Capricorn, Germany), MTT stain (Bio-World, USA), RPMI 1640 (Capricorn, Germany), Trypsin/EDTA (Capricorn, Germany), and TLC Plates (Silica gel F_{254}, 20 x 20 cm, thickness 2mm) (Merck, Germany).

Physical measurements

^{1}H & ^{13}C NMR spectra were recorded on a Bruker Varian / Inova 500 MHz (USA). Fourier transform infrared spectra (FT–IR) were given on a Shimadzu–8400S spectrophotometer (Germany) within a range of (4000 –200 cm^{-1}) by preparation of KBr discs. Melting point (MP) was recorded using an Electro-Thermal Stuart SMP 30 apparatus (U. K). The electronic spectra are measured by using a CECILL CE 7200 UV-Visible Spectrophotometer (U. K) by dissolving synthesised compounds in DMSO at concentration of (10^{-3} M).

Chemical Synthesis

Synthesis of 4,4`-Diformyldibenzo-18-Crown-6 Ether.

A mixture of dibenzo-18-crown-6 (1 g, 2.77 mmol), trifluoroacetic acid (4 mL), and hexamethylene tetraamine (1.6 g, 11.4 mmol) was stirred and refluxed overnight for 24 hours in a 100 mL round-bottomed flask at 90°C and ammonia was left to evaporate. The mixture was extracted with 25 mL ethanol (96%), and the extract was filtered and evaporated, TLC tested at the time reaction (R_f value=0.76; in 5:5 of MeOH / DCM). Concentration of the ethanol extract gave reddish-brown oil, which on cooling solidified to reddish-brown powder of the desired compound **(Table 1)** [23],[24].

Spectral data [FDB]. Reddish-brown powder; yield (1 g, 87%); melting point (198-199 °C); (FT-IR cm^{-1}) (KBr) **(Table 3)**: 3448.84 and 3429.55 ν (O-H Stretching), 3038.94 ν (C-H Stretching) $_{Aromatic}$, 2935.76, 2877.89 and 2847.03 ν (C-H Stretching) $_{Aliphatic}$, 1697.41 ν (C=O Stretching), 1593.25, 1512.24, 1438.94 and 1404.22 ν (C=C Stretching) $_{Aromatic}$, 1361.79 ν (C-H bending) $_{Aliphatic}$, 1265.35, 1203.62, 1176.62 and 1130.32 ν (C-O-C Stretching), 1057.03 ν (C-O Stretching). ^{1}H-NMR data (ppm), δH (500 MHz, DMSO-d6): δ = 3.82 (m, 8H), 4.04 (m, 8H), 6.88–7.30 (m, 6H), 9.8 (s, 2H); ^{13}C-NMR data (ppm), (DMSO-d6, 75MHz): δ = 191.96, 153.81, 148.70, 148.31, 148.23, 129.99, 126.57, 121.15, 112.76, 112.56, 112.18, 110.30, 69.35, 69.04, 68.95, 68.62, 67.96, 67.76.

Synthesis of 4,4`-di[9-(2-hydroxyethoxy) methyl]-2-(methylidene amino)-1,9-dihydro-6H-purin-6-one- [6,7,9,10,17,18,20,21]- Octa hydro- [b, k] dibenzo [1,4,7,10,13,16] hexaoxacyclooctadecine (Prodrug A1).

A hot stirred solution of acyclovir (0.450 g, 2 mmol), 40 mL methanol, was added to FDB (0.416 g, 1 mmol) were mixed in 100 mL round bottom flask. To the reaction mixture (8 drops) of glacial acetic acid were added as a catalyst. The reaction was reflexed with stirrer for 15 hours, and TLC tested the time reaction (R_f value=0.4; in 5:5 of MeOH / DCM). Then, the mixture was cooled overnight. The precipitate was filtered and purified by recrystallization from ethanol (96%)[25]. Light brown powder of the desired compound was collected **(Table 1).**

Spectral data [Prodrug A1]. Light brown powder; yield (0.66 g, 80%); melting point (230 °C); (FT-IR cm^{-1}) (KBr) **(Table 3)**: 3437.26 ν (O-H Stretching), 3050.22 ν (C-H Stretching) $_{Aromatic}$, 2931.90 and 2881.75 ν (C-H Stretching) $_{Aliphatic}$, 1679.27 ν (C=O Stretching, amide), 1646.36 and 1631.83 ν

(C=N Stretching), 1535.39 ν (C=C Stretching) $_{Aromatic}$, 1481.38 and 1384.94 ν (C-H bending) $_{Aliphatic}$, 1222.91, 1180.47 and 1111.03 ν (C-O-C Stretching), 1072.46 and 1010.73 ν (C-O Stretching). ^{1}H-NMR data (ppm), δH (500 MHz, DMSO-d6) **(Table 4)**: δ = 6.04 – 6.18 (HC=N); ^{13}C-NMR data (ppm), (DMSO-d6, 75MHz) **(Table 5)**: δ = 165, 157, 159, 153, 150, 140, 125, 120, 116, 110, 75, 70 and 59.

Synthesis of 4,4`-di-1-[3,4-dihydroxy-5-(hydroxymethyl) oxolan-2-yl]-4-[(E)-ethylideneamino] pyrimidin-2(1H)-one- [6,7,9,10,17,18,20,21]- Octa hydro- [b, k] dibenzo [1,4,7,10, 13, 16] hexaoxacyclooctadecine (Prodrug A2).

A hot stirred solution of cytarabine (0.486 g, 2 mmol), 40 mL methanol, was added to FDB (0.416 g, 1 mmol) were mixed in 100 mL round bottom flask. To the reaction mixture (8drops) of glacial acetic acid were added as a catalyst. The reaction was reflexed with stirrer for 15 hours, and TLC tested the time reaction (R_f value=0.7; in 3:7:5 drops of MeOH / DCM / NH_4OH). Then, the mixture was cooled overnight. The precipitate was filtered and purified by recrystallization from ethanol (96%)[25]. Off-white powder of the desired compound was collected **(Table 1).**

Spectral data [Prodrug A2]. Off-white powder; yield (0.37 g, 43%); melting point (189-191 °C); (FT-IR cm^{-1}) (KBr) **(Table 3)**: 3444.98 and 3425.69 ν (O-H Stretching), 3052.87 ν (C-H Stretching) $_{Aromatic}$, 2928.04, 2881.75, 2835.45 and 2754.44 ν (C-H Stretching) $_{Aliphatic}$, 1670.41 ν (C=O Stretching), 1644.55 and 1635.69ν (C=N Stretching), 1593.25 and 1512.24 ν (C=C Stretching) $_{Aromatic}$, 1438.94 and 1396.51 ν (C-H bending) $_{Aliphatic}$, 1269.20, 1172.76 and 1134.18 ν (C-O-C Stretching), 1057.03 ν (C-O Stretching). ^{1}H-NMR data (ppm), δH (500 MHz, DMSO-d6) **(Table 4)**: δ = 7.15 – 7.17 (HC=N); ^{13}C-NMR data (ppm), (DMSO-d6, 75MHz) **(Table 5):** δ = 181, 164, 160, 150, 142, 121, 111, 105, 100, 87, 75, 70, 69 and 60.

Synthesis of 4,4`-di-5-[2-chloro-6-(methylideneamino)-9H-purin-9-yl]-2-(hydroxymethyl) oxolan-3-ol- [6,7,9,10,17,18,20,21]- Octa hydro- [b, k] dibenzo [1,4,7,10,13,16] hexaoxacyclooctadecine (Prodrug A3).

A hot stirred solution of cladribine (0.570 g, 2 mmol), 40 mL methanol, was added to FDB (0.416 g, 1 mmol) were mixed in 100 mL round bottom flask. To the reaction mixture (8drops) of glacial acetic acid were added as a catalyst. The reaction was reflexed with stirrer for 15 hours, and TLC tested the time reaction (R_f value=0.83; in 3:7:5 drops of MeOH / DCM / NH_4OH). Then, the

mixture was cooled overnight. The precipitate was filtered and purified by recrystallization from ethanol (96%)[25]. Brown crystalline powder of the desired compound was collected **(Table 1)**. Spectral data [Prodrug A3]. Brown crystalline powder; yield (0.75 g, 79%); melting point (197-199 °C); (FT-IR cm^{-1}) (KBr) **(Table 3)**: 3448.84 and 3421.83 ν (O-H Stretching), 3016.93 ν (C-H Stretching) $_{Aromatic}$, 2928.04, 2881.75 and 2831.60 ν (C-H Stretching) $_{Aliphatic}$, 1657.03 ν (C=N Stretching), 1589.40 and 1512.24 ν (C=C Stretching) $_{Aromatic}$, 1438.94 and 1396.51 ν (C-H bending) $_{Aliphatic}$, 1269.20, 1176.62 and 1134.18 ν (C-O-C Stretching), 1057.03 ν (C-O Stretching). ^{1}H-NMR data (ppm), δH (500 MHz, DMSO-d6) **(Table 4)**: δ = 7.15 – 7.17 (HC=N); ^{13}C-NMR data (ppm), (DMSO-d6, 75MHz) **(Table 5)**: δ = 160, 159, 153, 152, 150, 140, 130, 125, 123, 111, 93, 89, 71, 70 and 61.

Anticancer Activity

Maintenance of Cell Cultures

THP-1 Cells were maintained in RPMI-1640 supplemented with 10% Fetal bovine serum, 100 units/mL penicillin, and 100 µg/mL streptomycin. Cells were passaged using Trypsin-EDTA reseeded at 80% confluence twice a week, and incubated at 37 °C [26], [27].

Cytotoxicity Assays

To determine the cytotoxic effect of starting materials and A1, A2 and A3 prodrugs, the MTT assay was done using 96-well plates [28],[29]. Cell lines were seeded at 1×10^4 cells/well. After 24 hrs. or a confluent monolayer was achieved, cells were treated with tested compounds at different concentrations. Cell viability was measured after 72 hrs. of treatment by removing the medium, adding 28 µL of 2 mg/mL solution of MTT and incubating the cells for 2.5 h at 37 °C. After removing the MTT solution, the crystals remaining in the wells were solubilized by the addition of 130 µL of DMSO followed by 37 °C incubation for 15 min with shaking[29]. The absorbency was determined on a microplate reader at 492 nm; the assay was performed in triplicate. The inhibition rate of cell growth (the percentage of cytotoxicity) was calculated as the following equation[30]: **Cytotoxicity = A-B/A*100,** where A is the optical density of control, and B is the optical density of the samples [31].

Results and Discussion

Chemistry

The three targeted new compounds were designed as carrier-mediated prodrugs in which certain dibenzo-18-crown-6 ether is formylated to produce 4,4`-Diformyldibenzo-18-Crown-6 Ether which is in turn linked to the desired starting materials as Schiff's bases to produce prodrug A1, prodrug A2 and prodrug A3. The characterization and the purity of the intermediates and the target compounds (appearance, melting points, percent yields and R_f values) were summarized in **Table (1)**. The functional groups of the synthesized compounds were identified by using FT-IR spectroscopy. UV electronic spectra was one technique have successfully characterized the new synthesized ligand and the chemical structures of targeted compounds were confirmed by using ^{1}H-NMR and ^{13}C-NMR spectroscopy.

Formylation of Dibenzo-18-Crown-6 Ether.

The formylation of dibenzo-18-crown-6 by using trifluoroacetic acid (as catalyst) and hexamine (as reagent and the formyl carbon source) in the presence of ethanol (as solvent) achieved by Duff formylation reaction. The first step including TFA bonds with hexamine and makes transforms into the more electrophile (carbocation ion) much easier around to attack the benzene ring. The ethylene oxide in the crown backbone attached to benzene ring at C-1 position is a strong pi donor group (OCH_2CH_3) and the formation of an anion adjacent to that group at C-1 is actually disfavoured leading to electron reppulsion, so placing the negative charge as far away from the pi-donating group as possible at the C-4 position is favorable. The alkoxyl groups are the electron-donating group responsible for both its activating properties and its ortho-para directing properties, for the intermediates leading to the ortho and para products, one of the contributing carbocation structures is tertiary. This structure is more stable than the others because the electrons on the methyl group can directly stabilize the electron deficient carbocation carbon. This stability is passed on to the resonance hybrid, which makes the intermediates for attack at the more stable than that for attack at the meta position. More stable intermediates mean lower energy transition states and faster reactions. A faster reaction means more product is formed through that pathway, giving an explanation why cis-trans isomer can be produced. The carbonyl

group is an electron withdrawing and meta-directing substituent with positive charge directly adjacent to the positive end of the carbonyl group's dipole. The energy of such an intermediate will be higher than carbonyl carbon, and the consequence is faster and more meta product is formed giving an explanation why cis-cis isomer can be produced [32]. The mechanism of duff formylation reaction was illustrated in **Scheme (1).**

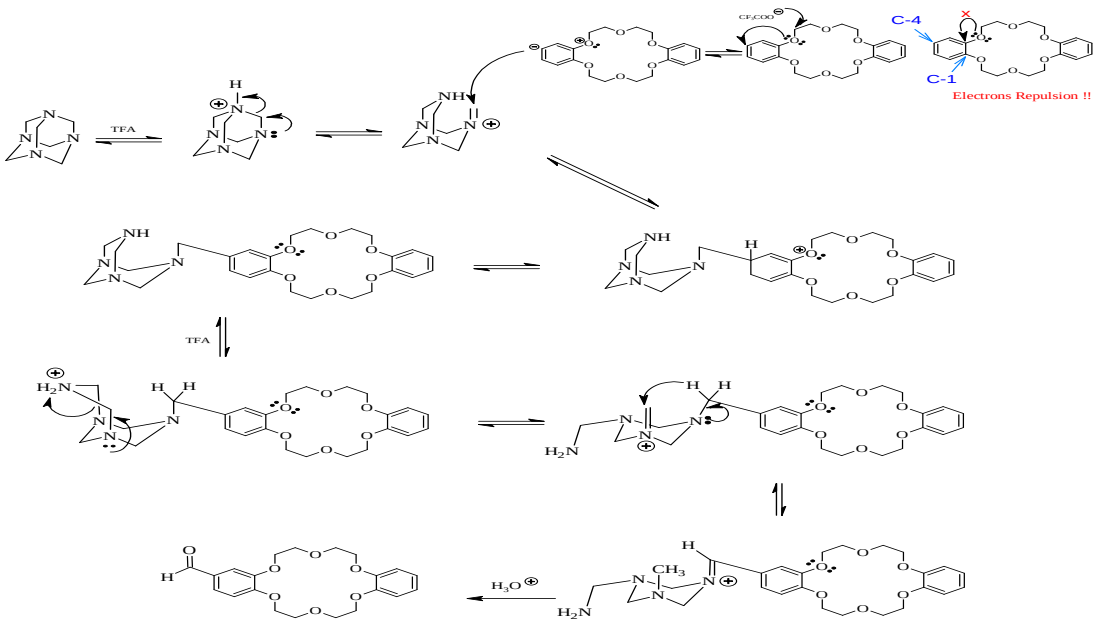

Scheme (1): General mechanism of Duff formylation reaction.

The Synthesis of Prodrugs A1, A2 and A3 as Schiff's bases

Schiff's bases are typically made by nucleophilic addition of primary amines and active carbonyl groups through a condensation reaction to form a hemiaminal, which is then dehydrated to produce an imine. Mechanistically, there are two processes in the creation of an imine. First, the amine nitrogen functions as a nucleophile, attacking the aldehyde or ketone's electrophilic carbonyl carbon. The nitrogen is then deprotonated, and the electrons from the N-H bond push the oxygen away from the carbon, leaving a product with a C=N double bond (an imine) and a displaced water molecule [33] as shown in **Scheme (2).** Acyclovir, cytarabine and cladribine are nucleoside antimetabolites which prepared as Schiff bases when these substances added to 4,4'-diformyldibenzo-18-crown-6 in the presence of methanol (as a solvent) and glacial acetic acid (as a catalyst) at certain conditions.

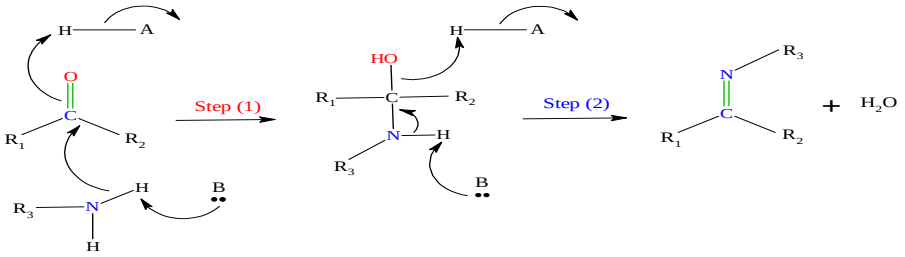

Scheme (2): General mechanism of the formation of Schiff's base (an imine).

Electronic spectra

All new Schiff's base prodrugs were scanned by a UV spectrophotometer with their parent compounds in equimolar concentration, there is a significant difference in (λ_{max}) as shown in **Table (2)**, thus making UV method relevant for our studies.

Fourier-Transform Infrared Spectra (FT-IR)

The FTIR spectra of the synthesized Schiff's base compounds and their intermediates were performed by the KBr disc method as shown in **Table (3)**.

^{1}H & ^{13}C -NMR Spectra

NMR Spectra for all prodrugs were performed in deuterated dimethyl sulfoxide (DMSO-d_6) as a solvent and tetramethyl saline (TMS) as an internal standard. In details, the data of ^{1}H & ^{13}C -NMR Spectra of all three Schiff's bases prodrugs shown below in **Table (4)** and **(5)**, respectively.

Table (2): The λ_{max} values of some starting materials and prodrugs.

Compound	λ_{max} values (nm)	Assignment
FDB	193.5 and 277.5; 205 and 229.5	Pi→Pi*, *n*→Pi*of carbonyl (C=O) group; Pi→Pi* of the aromatic system.
Prodrug A1	205.5, 229.5, 71.5 and 304; 355.5	Pi→Pi* of the aromatic system; Pi→Pi* of the (C=N) group.
Prodrug A2	206.5, 225.5, 258 and 302.5; 335.5	Pi→Pi* of the aromatic system; Pi→Pi* of the (C=N) group.
Prodrug A3	205.5 and 283; 318	Pi→Pi* of the aromatic system; Pi→Pi* of the (C=N) group.

Table (1): The physicochemical parameters of the target compounds and their intermediates.

Compound	Molecular Formula	Molecular Weight (g/mol)	Appearance	Yield (%)	Melting Point (°C)	R_f value	Eluent system
DB-18-C-6	$C_{20}H_{24}O_6$	360.401	White-like cotton fluffy powder	_	161-163	0.91	MeOH / DCM 5:5
FDB	$C_{22}H_{24}O_8$	416.4211	Reddish-brown powder	87	198-199	0.76	MeOH / DCM 5:5
Acyclovir (ACV)	$C_8H_{11}N_5O_3$	225.2046	White crystalline powder	_	255-257	0.51 0.26	MeOH / DCM 5:5 Hexane / EtOH 7:3
Prodrug A1	$C_{38}H_{42}N_{10}O_{12}$	830.7998	Light brown powder	80	230	0.4	MeOH / DCM 5:5
Cytarabine (Ara-C)	$C_9H_{13}N_3O_5$	243.2166	White to off-white crystalline powder	_	212-213	0.63 0.94	MeOH / DCM 5:5 DCM / Water / EtOH 7:2:1
Prodrug A2	$C_{40}H_{46}N_6O_{16}$	866.8238	Off-white powder	43	189-191	0.7	MeOH / DCM / NH_4OH 3:7:5 drops
Cladribine (CLD)	$C_{10}H_{12}ClN_5O_3$	285.687	Off-white crystalline powder	_	307	0.55	$CHCl_3$ / MeOH 5:5
Prodrug A3	$C_{42}H_{44}Cl_2N_{10}O_{12}$	951.7645	Brown crystalline powder	79	197-199	0.83	MeOH / DCM / NH_4OH 3:7:5 drops

Table (3): The data and vibrational mode description of FTIR spectra of all prodrugs.

Compounds	Vibrational mode (υ^{-1})										
	O-H Stretching	**C-H** Stretching (Aromatic)	**C-H** Stretching (Aliphatic)	**C=O** Stretching	**C=N** Stretching	**C=C** Stretching (Aromatic)	**C-H** bending (Aliphatic)	**C-O-C** Stretching	**C-O** Stretching	**C-H** bending (Out plane) (Aromatic)	**C-O-H** bending (Out plane)
FDB	3448.84 (b) 3429.55 (b)	3038.94 (w)	2935.76 (w) 2877.89 (w)	1697.41 (s)	–	1593.25 1512.24 1438.94 1404.22	1361.79	1265.35 1203.62 1176.62 1130.32	1057.03	999.16 725.26	659.68
Prodrug A1	3437.26 (w)	3050.22 (w)	2931.90 (w) 2881.75 (w)	1679.27 (m) (amide)	1646.36 (b, s) 1631.83 (b, s)	1535.39 (w, b)	1481.38 1384.94	1222.91 1180.47 1111.03	1072.46 1010.73	898.86 756.12	682.82 628.81
Prodrug A2	3444.98 3425.69	3052.87 (w)	2928.04 2881.75 2835.45 2754.44	1670.41	1644.55 1635.69	1593.25 1512.24	1438.94 1396.51	1269.20 1172.76 1134.18	1057.03	999.16 744.55	659.68
Prodrug A3	3448.84 3421.83	3016.93 (w)	2928.04 2881.75 2831.60	–	1657.03 (s)	1589.40 1512.24	1438.94 1396.51	1269.20 1176.62 1134.18	1057.03	999.16 744.55	663.53 628.81
S=sharp; m=medium; w=weak; b=broad											

Table (4): ^{1}H-NMR spectra of all Schiff's bases prodrugs.

Compound	Type of proton	chemical shift (δ) in (ppm)	Description of proton
Prodrug A1	H-C-H	1.03 – 1.06	Protons of CH_2 group at position 11;
		1.16 – 1.23	Protons of CH_2 group at position 12;
		2.33 – 2.42	Protons of CH_2 group at position 17;
		2.54 – 2.7	Protons of CH_2 group at position 16;
		4.18 – 4.31	Protons of CH_2 group at position 10
	C-H	4.06 – 4.10	Proton of CH group at position 8;
		5.92 – 5.95	Proton of CH group at position 15;
		6.22 – 6.33	Proton of CH group at position 13 and 14
	HC=N	6.04 – 6.18	Proton of Schiff's base (C=N) group
	N-H	12.5	Proton of (N-H) group at position 1
	O-H	3.59 – 3.61	Proton of alcoholic OH group
Prodrug A2	H-C-H	3.86	Protons of CH_2 group at position 5';
		4.18 – 4.19	Protons of CH_2 group of the crown backbone
	C-H	4.05	Proton of CH group at position 4';
		4.14 – 4.15	Proton of CH group at position 3';
		5.76	Proton of CH group at position 2';
		6.85 – 6.87	Proton of CH group at position 5;
		6.91 – 6.92	Proton of CH group at position 1';
		7.53 – 7.55	Proton of CH group at position 5;
		7.37	Proton of CH group of the aromatic ring of crown backbone
	HC=N	7.15 – 7.17	Proton of Schiff's base (C=N) group
	O-H	3.25	Proton of alcoholic OH group at position 6';
		9.83	Proton of OH group at position 2'and 3'
Prodrug A3	H-C-H	3.86 – 3.87	Protons of CH_2 group at position 5';
		4.14 – 4.20	Protons of CH_2 group of the crown backbone;
	C-H	4.05	Proton of CH group at position 4';
		5.75	Proton of CH group at position 3';
		6.91 – 6.93	Proton of CH group at position 1';
		7.53 – 7.55	Proton of CH group at position 2;
		7.37	Proton of CH group of the aromatic ring of crown backbone
	HC=N	7.15 – 7.17	Proton of Schiff's base (C=N) group
	O-H	6.84 – 6.88	Proton of alcoholic OH group at position 6';
		9.83	Proton of OH group at position 3'

Table (5): ^{13}C-NMR spectra of all Schiff's bases prodrugs.

Compound	chemical shift (δ) in (ppm)	Description of carbon environment
Prodrug A1	165	Carbon environment at position 6;
	157-159	Carbon environment at position 2;
	153	C=N of an imine group;
	150	Carbon environment at position 4;
	140	Carbon environment at position 15;
	125	Carbon environment at position 8;
	120	Carbon environment at position 13;
	116	Carbon environment at position 5;
	110	Carbon environment at position 14;
	75	Carbon environment at position 16 or 10;
	70	Carbon environment at position 17 or 11;
	59	Carbon environment at position 12.
Prodrug A2	181	Carbon environment at position 2;
	164	Carbon environment at position 4;
	160	C=N of an imine group;
	150	Carbon environment at position 15;
	142	Carbon environment at position 6;
	121	Carbon environment at position 13;
	111	Carbon environment at position 14;
	105	Carbon environment at position 5;
	100	Carbon environment at position 1';
	87	Carbon environment at position 4';
	75	Carbon environment at position 2' OR 3';
	70	Carbon environment at position 16;
	69	Carbon environment at position 17;
	60	Carbon environment at position 5';
Prodrug A3	160	Carbon environment at position 1;
	159	C=N of an imine group;
	153	Carbon environment at position 5;
	152	Carbon environment at position 13;
	150	Carbon environment at position 3;
	140	Carbon environment at position 11;
	130	Carbon environment at position 12;
	125	Carbon environment at position 6;
	123	Carbon environment at position 9;
	111	Carbon environment at position 8;
	93	Carbon environment at position 2;

	89	Carbon environment at position 7;
	71	Carbon environment at position 14;
	70	Carbon environment at position 15;
	61	Carbon environment at position 10.

Anticancer Activity

The cytotoxic effects of acyclovir, cytarabine, cladribine and their related prodrugs A1, A2 and A3 against cancer cells were studied. These chemicals' anticancer properties were examined by looking at their capacity to stop cancer cells from multiplying. The findings of this investigation revealed a high level of cytotoxic activity of all starting materials and their prodrugs against the human cancer cell lines as shown in **Figures (2 to 4).** The findings imply that all of the chemicals examined have the capacity to inhibit the proliferation of cancer cell lines in a concentration-dependent way. Further to this, insignificant differences were found between acyclovir (ACV) and its prodrug (A1) as seen in **Figure (2).** Regarding cytarabine and cladribine, significant differences between the cytotoxic activities of the starting compounds and their prodrugs at all the tested concentrations except at 3.1 ug/ml as shown in **Figures (3) and (4).**

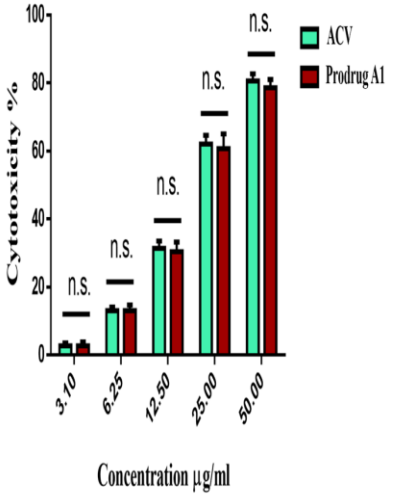

Figure(2):Cytotoxic effect of ACV & Prodrug A1 in THP-1 cells.

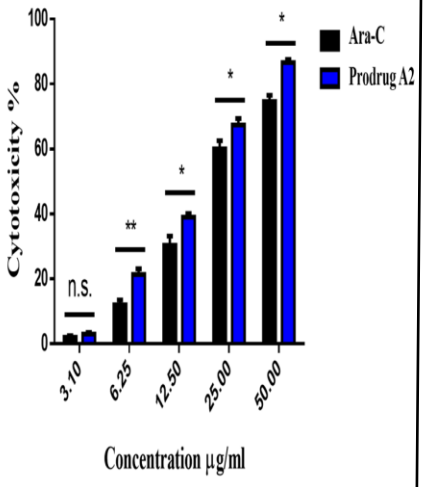

Figure(3):Cytotoxic effect of Ara-C & Prodrug A2 in THP-1 cells.

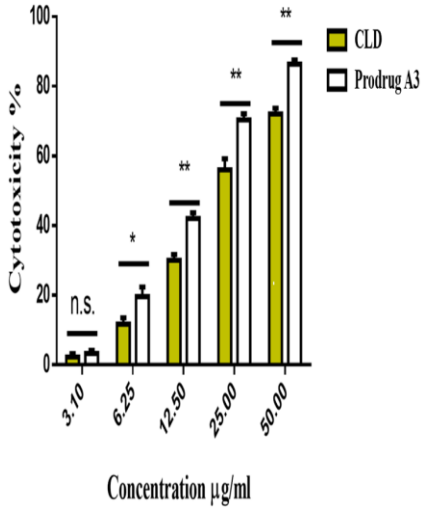

Figure(4): Cytotoxic effect of CLD & Prodrug A3 in THP-1 cells.

References:

[1] D. Zhou *et al.*, "Specific Host-Guest Interactions in the Crown Ether Complexes with K+and NH4+Revealed from the Vibrational Relaxation Dynamics of the Counteranion," *J. Phys. Chem. B*, vol. 124, no. 41, pp. 9154–9162, 2020, doi: 10.1021/acs.jpcb.0c07032.

[2] C. J. Pedersen, "Cyclic polyethers and their complexes with metal salts," *J. Am. Chem. Soc.*, vol. 89, no. 26, pp. 7017–7036, 1967, doi: 10.1021/ja01002a035.

[3] T. Ogoshi and T. Yamagishi, "Chapter 1 Historical Background of Macrocyclic Compounds," in *Pillararenes*, Y. T. C. 1 H. B. of M. C. I. P. T. R. S. of C. 2016:1-22. doi:10. 1039/978178262232.-00001 1. Ogoshi T, Ed. The Royal Society of Chemistry, 2016, pp. 1–22.

[4] G. T. Williams, C. J. E. Haynes, M. Fares, C. Caltagirone, J. R. Hiscock, and P. A. Gale, "Advances in applied supramolecular technologies," *Chem. Soc. Rev.*, vol. 50, no. 4, pp. 2737–2763, 2021, doi: 10.1039/d0cs00948b.

[5] L. A. Viarengo-Baker, L. E. Brown, A. A. Rzepiela, and A. Whitty, "Defining and navigating macrocycle chemical space," *Chem. Sci.*, vol. 12, no. 12, pp. 4309–4328, 2021, doi: 10.1039/d0sc05788f.

[6] P. M. G. Löffler *et al.*, "Lipidated Polyaza Crown Ethers as Membrane Anchors for DNA-Controlled Content Mixing between Liposomes," *Sci. Rep.*, vol. 9, no. 1, pp. 1–11, 2019, doi: 10.1038/s41598-019-49862-y.

[7] Z. Rapi, T. Nemcsok, P. Bagi, G. Keglevich, and P. Bakó, "Synthesis of chiral crown ethers derived from d-galactose and their application in enantioselective reactions," *Tetrahedron*, vol. 75, no. 30, pp. 3993–4004, 2019, doi: https://doi.org/10.1016/j.tet.2019.06.020.

[8] H.-F. Wang and S.-P. Wu, "Highly selective fluorescent sensors for mercury(II) ions and their applications in living cell imaging," *Tetrahedron*, vol. 69, no. 8, pp. 1965–1969, 2013, doi: https://doi.org/10.1016/j.tet.2012.12.075.

[9] R. Mohammadzadeh Kakhki, “Application of crown ethers as stationary phase in the chromatographic methods,” *J. Incl. Phenom. Macrocycl. Chem.*, vol. 75, no. 1–2, pp. 11–22, 2013, doi: 10.1007/s10847-012-0158-0.

[10] D. Parker and S. J. Butler, “Macrocycles. Construction, Chemistry and Nanotechnology Applications. By Frank Davis and Séamus Higson.,” *Angew. Chemie Int. Ed.*, vol. 50, no. 50, pp. 11842–11842, 2011, doi: 10.1002/anie.201105634.

[11] E. M. M. Abdelraheem, S. Shaabani, and A. Dömling, “Artificial Macrocycles.,” *Synlett*, vol. 29, no. 9, pp. 1136–1151, Jun. 2018, doi: 10.1055/s-0036-1591975.

[12] J. Mallinson and I. Collins, “Macrocycles in new drug discovery,” *Future Med. Chem.*, vol. 4, no. 11, pp. 1409–1438, 2012, doi: 10.4155/fmc.12.93.

[13] S. D. Jagadale, “Synthesis of Crown Ethers Contaning Nitrogen Oxygen and Sulphur Atoms,” p. 243, 2014, [Online]. Available: http://hdl.handle.net/10603/135621.

[14] G. Chehardoli and A. Bahmani, “The role of crown ethers in drug delivery,” *Supramol. Chem.*, vol. 31, no. 4, pp. 221–238, 2019, doi: 10.1080/10610278.2019.1568432.

[15] Z. Niu, G. K. Murakonda, R. Jarubula, and M. Dai, “Fabrication of Graphene oxide-Fe3O4 nanocomposites for application in bone regeneration and treatment of leukemia,” *J. Drug Deliv. Sci. Technol.*, vol. 63, p. 102412, 2021, doi: https://doi.org/10.1016/j.jddst.2021.102412.

[16] T. Yokoyama and M. Mizuguchi, “Crown Ethers as Transthyretin Amyloidogenesis Inhibitors,” *J. Med. Chem.*, vol. 62, no. 4, pp. 2076–2082, 2019, doi: 10.1021/acs.jmedchem.8b01700.

[17] P. W. J. Morrison *et al.*, “Crown Ethers: Novel Permeability Enhancers for Ocular Drug Delivery?,” *Mol. Pharm.*, vol. 14, no. 10, pp. 3528–3538, 2017, doi: 10.1021/acs.molpharmaceut.7b00556.

[18] I. Guberović *et al.*, “Crown ethers reverse P-glycoprotein-mediated multidrug resistance in cancer cells,” *Sci. Rep.*, vol. 8, no. 1, pp. 1–14, 2018, doi: 10.1038/s41598-018-32770-y.

[19] A. Kajal, S. Bala, S. Kamboj, N. Sharma, and V. Saini, "Schiff Bases: A Versatile Pharmacophore," *J. Catal.*, vol. 2013, no. Mic, pp. 1–14, 2013, doi: 10.1155/2013/893512.

[20] M. F. Yesmin, S. Hossain, S. Nasira, and N. Uddin, "Cu (II) and Ni (II) Complexes of Schiff Base: Synthesis, Characterization and Antibacterial Activity," *Int. J. Adv. Res. Chem. Sci.*, vol. 7, no. 1, 2020, doi: 10.20431/2349-0403.0701002.

[21] E. Hejchman *et al.*, "Design, synthesis, and biological activity of Schiff bases bearing salicyl and 7-hydroxycoumarinyl moieties," *Monatshefte fur Chemie*, vol. 150, no. 2, pp. 255–266, 2019, doi: 10.1007/s00706-018-2325-5.

[22] D. Chaturvedi and M. Kamboj, "Role of Schiff Base in Drug Discovery Research," *Chem. Sci. J.*, vol. 7, no. 2, pp. 7–8, 2016, doi: 10.4172/2150-3494.1000e114.

[23] S. Jagadale, "Synthesis of Dibenzothiazolyldibenzo-18-Crown-6 and its Applications in Colorimetric Recognition of Palladium and as Antimicrobial Agent," *J. Heterocycl. Chem.*, 2015, doi: 10.1002/jhet.2561.

[24] P. P. Kapupara, S. P. Dholakia, V. P. Patel, and B. N. Suhagia, "Journal of Chemical and Pharmaceutical Research preparations," *J. Chem. Pharm. Res.*, vol. 3, no. 4, pp. 287–294, 2011.

[25] H. Salih Abood, A. Abdullah, and Z. Wrewish, "Synthesis, characterization and antibacterial studies of Schiff bases of acyclovir," *Int. J. Res. Pharm. Sci.*, vol. 11, pp. 411–415, 2020, doi: 10.26452/ijrps.v11i1.1835.

[26] K. S. Khashan, G. M. Sulaiman, S. A. Hussain, T. R. Marzoog, and M. S. Jabir, "Synthesis, characterization and evaluation of anti-bacterial, anti-parasitic and anti-cancer activities of aluminum-doped zinc oxide nanoparticles," *J. Inorg. Organomet. Polym. Mater.*, vol. 30, no. 9, pp. 3677–3693, 2020.

[27] M. Jabir *et al.*, "Linalool-Loaded Glutathione-Modified Gold Nanoparticles Conjugated with CALNN Peptide as Apoptosis Inducer and NF-κB Translocation Inhibitor in SKOV-3 Cell Line," *Int. J. Nanomedicine*, vol. 15, p. 9025, 2020.

[28] M. S. Jabir, U. M. Nayef, W. K. Abdulkadhim, and G. M. Sulaiman, “Supermagnetic Fe3O4-{PEG} nanoparticles combined with {NIR} laser and alternating magnetic field as potent anti-cancer agent against human ovarian cancer cells,” *Mater. Res. Express*, vol. 6, no. 11, p. 115412, Nov. 2019, doi: 10.1088/2053-1591/ab50a0.

[29] A. G. Al-Ziaydi, A. M. Al-Shammari, M. I. Hamzah, H. S. Kadhim, and M. S. Jabir, “Newcastle disease virus suppress glycolysis pathway and induce breast cancer cells death,” *VirusDisease*, vol. 31, no. 3, pp. 341–348, 2020, doi: 10.1007/s13337-020-00612-z.

[30] M. S. Jabir *et al.*, “Green synthesis of silver nanoparticles using Annona muricata extract as an inducer of apoptosis in cancer cells and inhibitor for NLRP3 inflammasome via enhanced autophagy,” *Nanomaterials*, vol. 11, no. 2, pp. 1–22, 2021, doi: 10.3390/nano11020384.

[31] H. M. Waheeb, G. M. Sulaiman, and M. S. Jabir, “Effect of hesperidin conjugated with golden nanoparticles on phagocytic activity: In vitro study,” *AIP Conf. Proc.*, vol. 2213, no. March, 2020, doi: 10.1063/5.0000159.

[32] K. Mcmichael, “Organic Chemistry - a ‘Carbonyl Early’ Approach,” pp. 37–39, 2021, [Online]. Available: https://libretexts.org.

[33] U. Sani, H. U. Na’ibi, and S. A. Dailami, “In vitro antimicrobial and antioxidant studies on N-(2- hydroxylbenzylidene) pyridine -2-amine and its M(II) complexes,” *Niger. J. Basic Appl. Sci.*, vol. 25, no. 1, p. 81, 2018, doi: 10.4314/njbas.v25i1.11.